https://revistas.ucr.ac.cr/index.php/ingenieria/index
www.ucr.ac.cr / ISSN: 2215-2652

Ingeniería

Revista de la Universidad de Costa Rica

JULIO/DICIEMBRE 2023 - VOLUMEN 33 (2)

DOI: 10.15517/ri.v33i2.52390
Ingeniería 33(2): 1-16, Julio-Diciembre, 2023. ISSN: 2215-2652. San José, Costa Rica

Experimental Testing of Wood Framed Walls with Available Materials in Costa Rica

Ensayos experimentales de muros de marcos de madera con materiales disponibles en Costa Rica

Guillermo González Beltrán
Universidad de Costa Rica, San José, Costa Rica
e-mail: guillermo.gonzalez@ucr.ac.cr
Código Orcid: 0000-0002-3467-6346

Recibido: *7 de setiembre 2022* **Aceptado:** *10 de enero 2023*

Abstract

This paper presents a research study about timber shear walls, with materials commercially available in Costa Rica. With new developments in engineered timber, the Costa Rican Seismic Code included a chapter on timber structures, defining diaphragms and shear walls as part of the lateral resisting system. A research study was then carried out, with the objective of determining the structural behavior of a typical shear wall. Twelve specimens were constructed and tested, varying the nail spacing and anchorage system. The specimens were tested with monotonic and cyclic loading procedures according to ASTM E564 and ASTM E2126 respectively. It was found that the specimens can develop an adequate shear strength and stiffness if the end studs are adequately anchored to the foundation. These results are an important input for the Costa Rican Seismic Code and for the development of engineered timber in Costa Rica.

Keywords:
Cyclic testing of wood framed walls, Ductility of wood framed walls, Monotonic testing of wood framed walls, Timber shear walls, Wood framed walls.

Resumen

Este artículo presenta una investigación sobre muros de cortante de madera, con materiales disponibles comercialmente en Costa Rica. Con nuevos desarrollos en la ingeniería de la madera, el Código Sísmico de Costa Rica incluyó un capítulo de estructuras de madera y definió diafragmas y muros de corte de madera como parte del sistema de resistencia lateral. Debido a lo anterior, se llevó a cabo un estudio experimental, con el objetivo de determinar el comportamiento estructural de un muro de cortante típico. Se construyeron doce especímenes de ensayo, variando el espaciamiento de los clavos y el sistema de anclaje. Los especímenes se ensayaron ante carga monotónica y cíclica, según los procedimientos de las normas ASTM E564 y ASTM E2126, respectivamente. Se encontró que los especímenes pueden desarrollar una capacidad y rigidez adecuadas, siempre y cuando los postes extremos se fijen a la fundación. Estos resultados son un insumo importante para el Código Sísmico de Costa Rica y para el desarrollo de la ingeniería de la madera en Costa Rica.

Palabras clave:
Ductilidad de muros con marcos de madera, Ensayos cíclicos de paredes con marcos de madera, Ensayos monotónicos de paredes con marcos de madera, Muros con marcos de madera, Muros de cortante de madera.

1. INTRODUCTION

In Costa Rica, timber was widely used for construction during the first half of the 20th century. However, with the arrival of the masonry concrete block and the unconscious felling of native trees, the use of timber in buildings diminished rapidly. During the second half of the 20th century, timber in construction was left to finishes such as floors, roofs, decks, skirting, stairs and the like. During the decades of the 80's and 90's, reforestation efforts made in different parts of the country provided sources of timber construction purposes which are still available today. As not all the demand is supplied from native forests and plantations, in recent years, increasing amounts of lumber and plywood are imported from different countries, such as Chile, China, United States, Argentina and Brazil. A few timber companies started to grow and produce timber for construction. In 2002, the Costa Rican Seismic Code included a chapter on structural timber. It was a chapter of two pages that gave a few indications on structural design of timber, mostly referencing to other documents. In 2010, the new chapter on timber structures expanded to twenty pages. In this chapter, wood framed diaphragms and shear walls were introduced. The given specifications are based on AF&PA [1]. There are also several requirements that are based on CEN [2]. The purpose of this paper is to present research carried out in Costa Rica, regarding wood framed walls, constructed with materials available in Costa Rica. The objective of this research is to verify whether the provisions given in the Costa Rican Seismic Code are suitable for the available materials. Hence, an experimental program was developed, in which twelve wood framed shear walls were constructed and tested at the facilities of the National Laboratory for Materials and Structural Models of the University of Costa Rica. In the first part of the program, six specimens were tested without hold-down anchors [3], [4]. During the second part, other six specimens were tested with hold-down anchors [5], [6]. The idea was to obtain a lower and higher strength boundary for both conditions, respectively, and compare them with strength design.

Research on wood frame shear walls has been extensively carried out, especially on those regions where they are part of the typical building system. The design methods and code specifications are based on the knowledge acquired in those studies. For instance, in the last five years, the following investigations among others can be mentioned. Branco *et al*. investigated the influence of sheathing panels and hold down anchors in the structural behavior of light framed walls [7]. Using an analytical model, they could predict the behavior with an error of approximately 24 % higher for the experimental values. Nagase *et al*. evaluated the performance of a plywood to timber connection with nails or screws under cyclic loading [8]. With this study, they found out the lifetime failures of the connection and could estimate the load – displacement relationship by combining the yield mode theory and failure lifetimes. Dhonju did his doctoral research on a parametric study on wood framed walls [9]. He carried out several tests on wood framed walls subjected to horizontal loads, varying fastener size and spacing, wall length, studs and plates configurations and vertical load. Among several conclusions, he found out that the spacing of the fasteners has more influence on the shear strength when subjected to vertical load. However, the stiffness is more affected by fastener spacing when no vertical load is applied. Also, the results from the recently developed shear wall called "Mid-ply wall" showed better strength and stiffness than the standard walls. Shadravan *et al*. conducted research on wood framed walls

in which they varied stud spacing, nail type and spacing, anchor bolt spacing and washer size, and base plate [10]. The results showed that decreasing the anchor bolt spacing from 1.8 m to 0.9 m and using double bottom plates increased the wall shear strength 122 %. Orellana *et al*. did an investigation on the structural behavior of wood frame shear walls subjected to horizontal loads simultaneously with high compressive loads, simulating the conditions for midrise buildings [11]. They found out that the load carrying capacity, stiffness, energy dissipation and ductility ratio are higher when high compressive loads are present. Therefore, not considering the effects of gravitational loads and bending moments might be too conservative.

The results of this research will serve as the first set of data on wood shear walls built with local materials and is intended to promote wood construction in the country.

2. MATERIALS AND METHODS

2.1 Test specimens

A total of twelve test specimens were constructed, each of them consisting of 2.44 × 2.44 m wood framed walls with plywood sheathing. From the twelve specimens, six did not have hold-down anchors at the end studs (type A specimens), as mentioned above. These specimens did not have hold downs because one of the purposes was to show the effect in strength and stiffness of not having them at the end studs. However, it is not recommended to build these walls without the hold downs, especially in wind and seismic prone areas. The other six specimens did have hold-down anchors at the end studs (type B specimens). From each of the two specimen types, three were constructed with a constant nail spacing of 150 mm (specimen A1 or B1). The spacing for the other three was reduced to 100 mm (specimen A2 or B2). Monotonic loading was applied to one of each group of three specimens, whereas cyclic loading was applied to the other two (see TABLE I). Each wood frame consisted of five 2×4'' studs, spaced at 610 mm on center and 2×4'' top and bottom plates. It should be noted that the loading beam in the test setup acts as the collector for the tested wall, so in practice the upper plate (beam) shall be composed of two 2×4'' elements. On the other hand, the end studs (chords) were composed by one 2×4'' studs for comparison purposes between the specimens with and without hold down anchors. However, it is recommended to build these walls with at least two 2×4'' studs (chords) at the end of the wall, especially in wind and seismic prone areas. The wood frame species was radiate pine (*Pynus radiata*) from Chile. The sheathing consisted of two 1.22 × 2.44 m, 9 mm thick plywood utility boards on both sides of the frame. Fig. 1 shows the test specimen used in this research. The connectors were common nails with 3.64 mm in diameter and 70 mm in length (ASTM F1667). The hold-down anchors utilized for the end studs of type B specimen, were steel angles connected to the stud by twenty-five screws (6 mm in diameter, 4.8 mm in root diameter and 68 mm of penetration) and to the bottom plate by a bolt (25 mm in diameter and 190 mm in length, SAE Grade 5). Lower capacity steel angles were also installed on the rest of the studs.

TABLE I
DESCRIPTION OF TEST SPECIMENS

Specimen type	Hold-down anchors	Nail spacing at wall boundaries and panel edges [mm]	Loading protocol
A1M	NO	150	MONOTONIC
A1C-1	NO	150	CYCLIC
A1C-2	NO	150	CYCLIC
A2M	NO	100	MONOTONIC
A2C-1	NO	100	CYCLIC
A2C-2	NO	100	CYCLIC
B1M	YES	150	MONOTONIC
B1C-1	YES	150	CYCLIC
B1C-2	YES	150	CYCLIC
B2M	YES	100	MONOTONIC
B2C-1	YES	100	CYCLIC
B2C-2	YES	100	CYCLIC

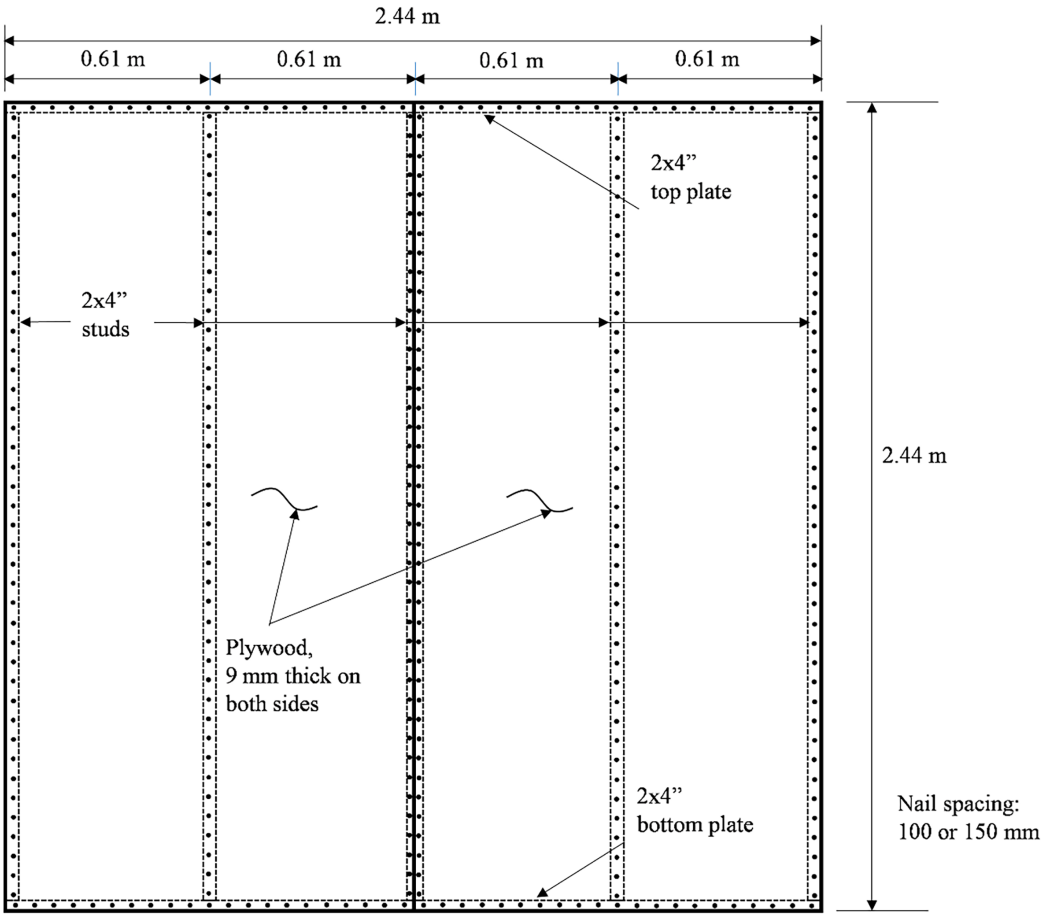

Fig. 1. Test specimen.

2.1 Experimental setup

The specimens were tested according to ASTM E564 [12] for the monotonic tests and ASTM E2126 [13] for the cyclic tests. The base of the wall was connected to the reaction floor via a steel beam. This beam was fixed to the reaction floor with anchor bolts. The bottom plate of the test specimen was attached to the bottom steel beam with bolts, 12.7 mm in diameter and 125 mm in length, spaced at 100 mm on center. More details of this connection can be found in [3] and [4]. The top of the wall was connected to a loading steel beam, which in turn was attached to the actuator. The latter was fixed to the reaction wall. Two steel frames prevented the beam from going sideways. The actuator transfers the load to the specimen through the loading steel beam, resulting in a distributed horizontal load at the top of the specimen. The specimen is forced to deform in its plane, including bending deformation of the chords (end studs), sheathing shear deformation, nail slip and anchor uplift. Vertical deformation of the specimen is possible due to the hinges at both ends of the actuator. In the case of the type A specimens, the load beam was connected to the wall by steel angles and bolts through the thickness of the wall lower than the top plate and, therefore, the horizontal load was transferred by bearing of the bolts in the sheathing on both sides. However, for type B specimens, which are stronger than type A specimens, this loaded system did not work and a new load beam was constructed, so that the loading transfer were achieved by connecting the load beam to the top plate with lag screws, 12.2 mm in diameter, 9.6 mm in root diameter and 109 mm long spaced at 115 mm on center. More details of these connections can be found in [5] and [6]. Fig. 2 shows a photograph of the experimental setup used in this research.

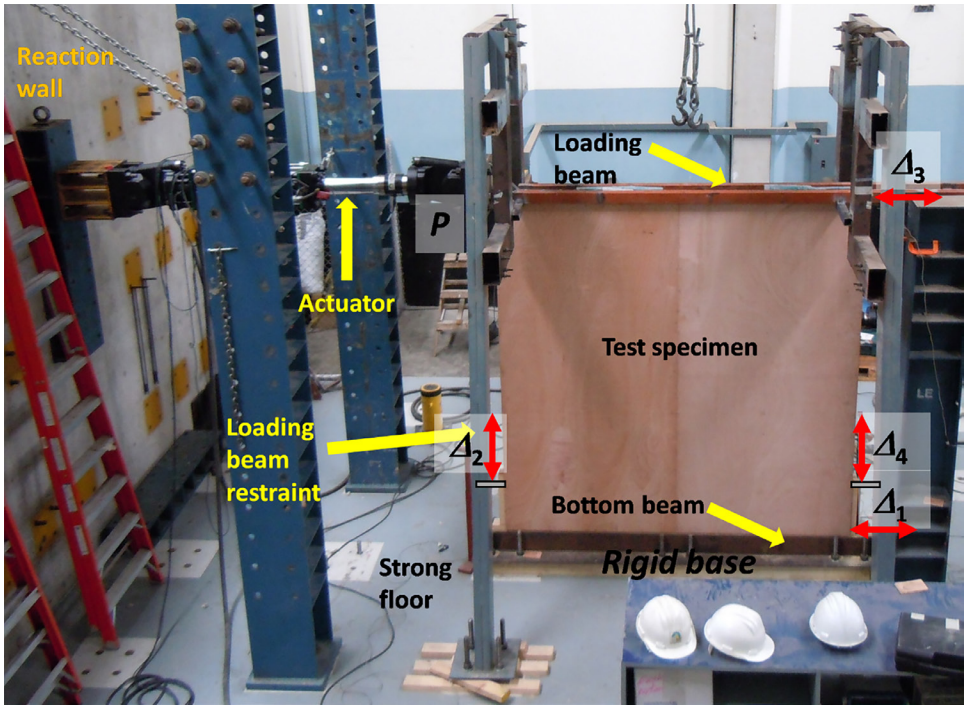

Fig. 2. Test setup.

Loading Protocol

The loading protocol for the monotonic tests consists of the following steps (based on ASTM E564):

1. Once all the measurement devices are checked, the specimen is loaded at 10 % of the anticipated maximum load. 2. The load is maintained for five minutes and then removed. 3. After five minutes, the initial data is recorded (displacements). 4. Then, the specimen can be loaded to several limit states, usually a certain amount of the maximum load, such as one third or two thirds. If this is the case, the load is maintained for five minutes and then removed. Step 3 is repeated. 5. The specimen is loaded until failure. Failure is defined when the peak load decreases 20 %.

The loading protocol for the cyclic tests is as follows (based on method B of ASTM E2126):

1. The specimen is subjected to five displacement cycles, based on the ultimate displacement (Δ_m) obtained from the monotonic test. The magnitude of each displacement cycle is 1.25, 2.5, 5, 7.5 and 10 % of Δ_m. 2. Afterwards, the displacement cycles are repeated three times at the following levels: 20, 40, 60, 80, 100 and 120 % of Δ_m. 3. If the specimen has not failed, the displacement cycle is incremented by 20 % and repeated three times. 4. If the specimen has not failed, step three is repeated until failure.

Instrumentation

The test specimen was instrumented with four LVDT's (Linear Variable Differential Transformers). LDVT 3 measures the horizontal displacement at the center of the top plate, LVDT 2 and LVDT 4 measure the vertical displacement of the end studs (chords) and LDVT 1 measures the horizontal displacement of the bottom plate (see Fig. 2). The actuator registered the applied load and displacement which is like the LVDT 3 measurement. The flexural and shear behavior of the specimen can be derived from the measurements mentioned above as will be explained in the next section.

3. RESULTS

3.1 Summary of results

The main results are shown in TABLE II. These values are calculated by assuming an equivalent energy elastic-plastic curve according to ASTM E2126 and is presented in the following section.

TABLE II
EXPERIMENTAL RESULTS

Specimen	v_{max} [kN/m]	v_Y [kN/m]	Δ_u [mm]	Δ_Y [mm]	G [kN/m]	D
A1M	8.70	8.07	56.4	9.52	2070	5.93
A1C-1	8.22	7.38	49.1	13.1	1595	3.75
A1C-2	8.16	6.95	41.4	9.37	2810	4.40
A2M	11.3	10.3	53.2	10.8	2290	4.95
A2C-1	11.1	9.77	49.6	13.4	3510	3.70
A2C-2	11.4	10.2	45.0	8.70	3000	5.18
B1M[1]	19.1	17.0	78.5	26.6	1566	2.95
B1C-1	17.6	15.4	67.0	12.6	3026	5.51
B1C-2	16.2	14.2	62.5	12.2	2821	5.10
B2M	22.1	19.9	69.1	10.9	4443	6.34
B2C-1	23.6	21.2	82.4	14.9	3430	5.53
B2C-2	24.7	21.7	77.0	18.4	2749	4.20

[1]This test specimen failed at the connection between the load beam and the top of the specimen and the reported values might not represent the expected behavior. These results are not considered when comparing with theoretical calculations.

Symbols: v_{max}: maximum unit shear load, v_y: yield unit shear load, Δ_u: ultimate displacement,Δ_y: yield displacement, G: apparent shear stiffness, D: ductility factor

3.2 Calculation procedure

From the load – displacement curves, the maximum load and ultimate displacement are obtained:

P_{max}: maximum applied load during test, kN. Δ_u: displacement at failure or at $0.8P_{max}$ after P_{max} has been reached, mm. The area under the envelope curve (A) up to Δ_u is estimated first (see Fig. 3 and Fig. 4).

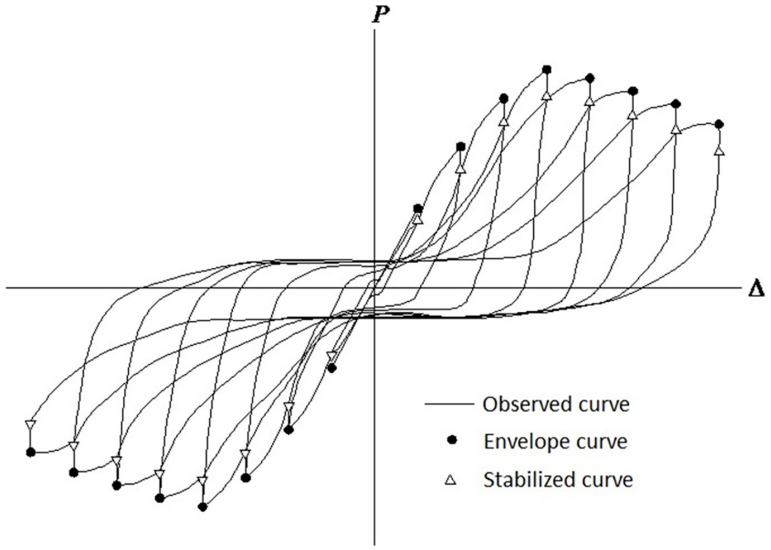

Fig. 3. Envelope curve.

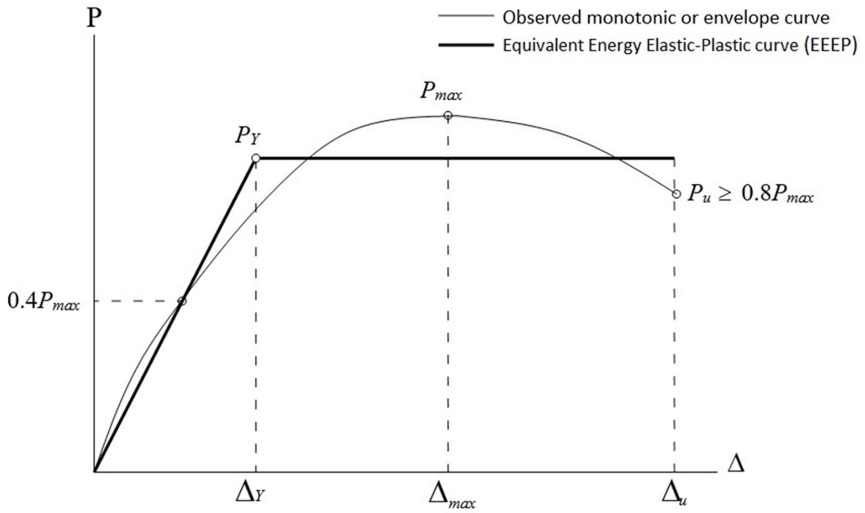

Fig. 4. Representation of the EEEP curve.

The elastic stiffness is assumed to be:

$$K_e = \frac{0.4P_{max}}{\Delta_e} \quad \text{Where } \Delta_e \text{ is the displacement at } 0.4P_{max}. \tag{1}$$

The yield load is calculated assuming an equivalent energy elastic-plastic curve (EEEP). For the cyclic load tests, an envelope curve is obtained from the maximum points in the first cycle of each displacement. This is done for the positive and negative curves (see Fig. 3). Once the envelope curves are drawn, the EEEP curve is defined (see Fig. 4). Once K_e is calculated, the yield load (P_Y) is obtained from:

$$P_Y = \left(\Delta_u - \sqrt{\Delta_u{}^2 - \frac{2A}{K_e}}\right) K_e \tag{2}$$

The yield displacement is then calculated by:

$$\Delta_Y = \frac{P_Y}{K_e} \tag{3}$$

The ductility factor D is obtained from:

$$D = \frac{\Delta_u}{\Delta_Y} \tag{4}$$

The unit shear loads (v_{max} and v_Y) are obtained by dividing the maximum and yield loads (P_{max} and P_Y) by the length of the wall (2.44 m). The apparent shear stiffness (includes bending deformation of the end posts, panel shear deformation, nail slip and anchor uplift) is estimated by:

$$G = k_e \frac{h}{b} \tag{5}$$

The displacement Δ considered in the calculations, corresponds to Δ_3-Δ_1 according to Fig. 2.

3.3 Load – displacement curves

Fig. 5 and Fig. 6 present the load – displacement curves obtained from each of the tested specimens.

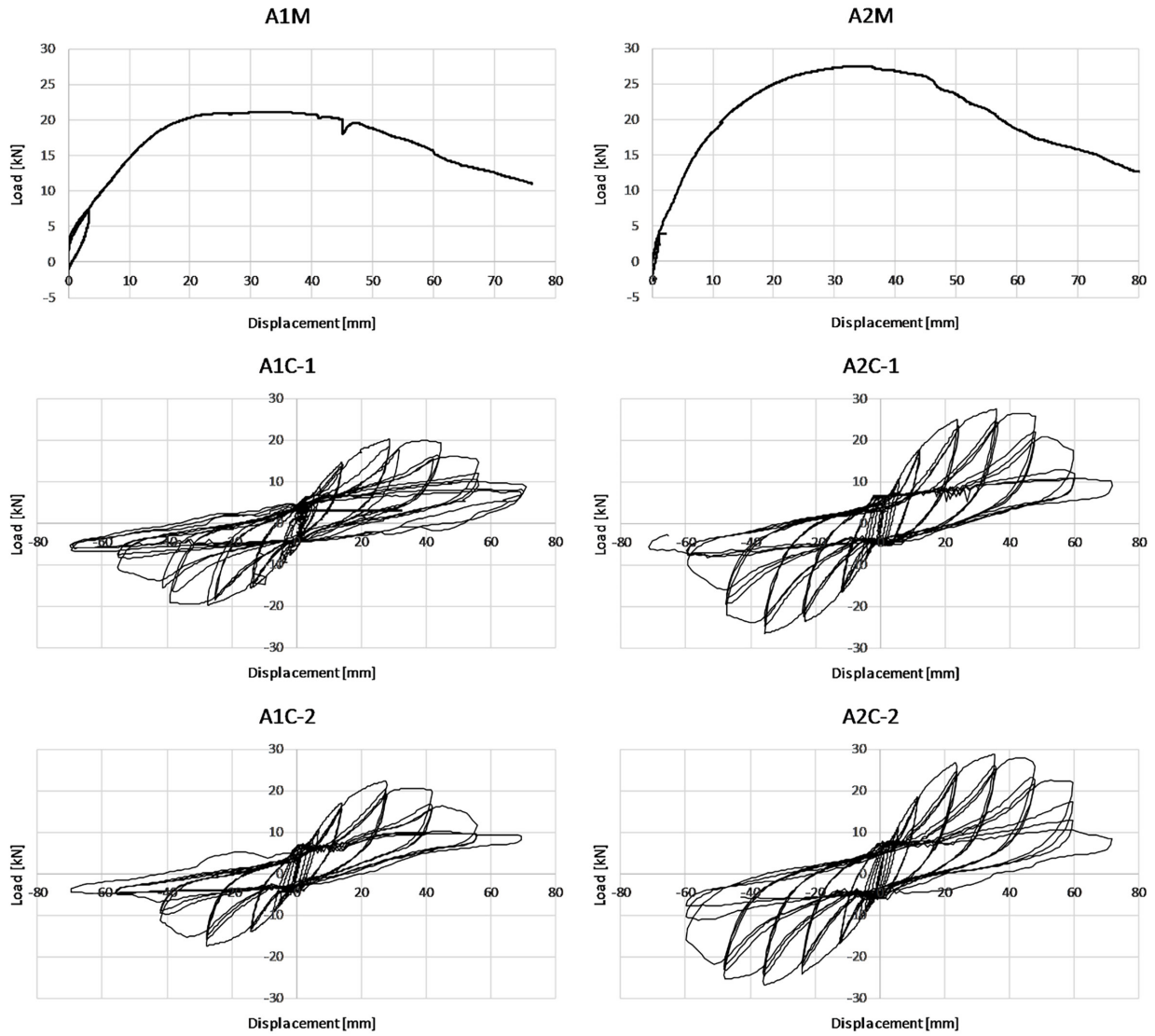

Fig. 5. Load – displacement curves for type A specimens.

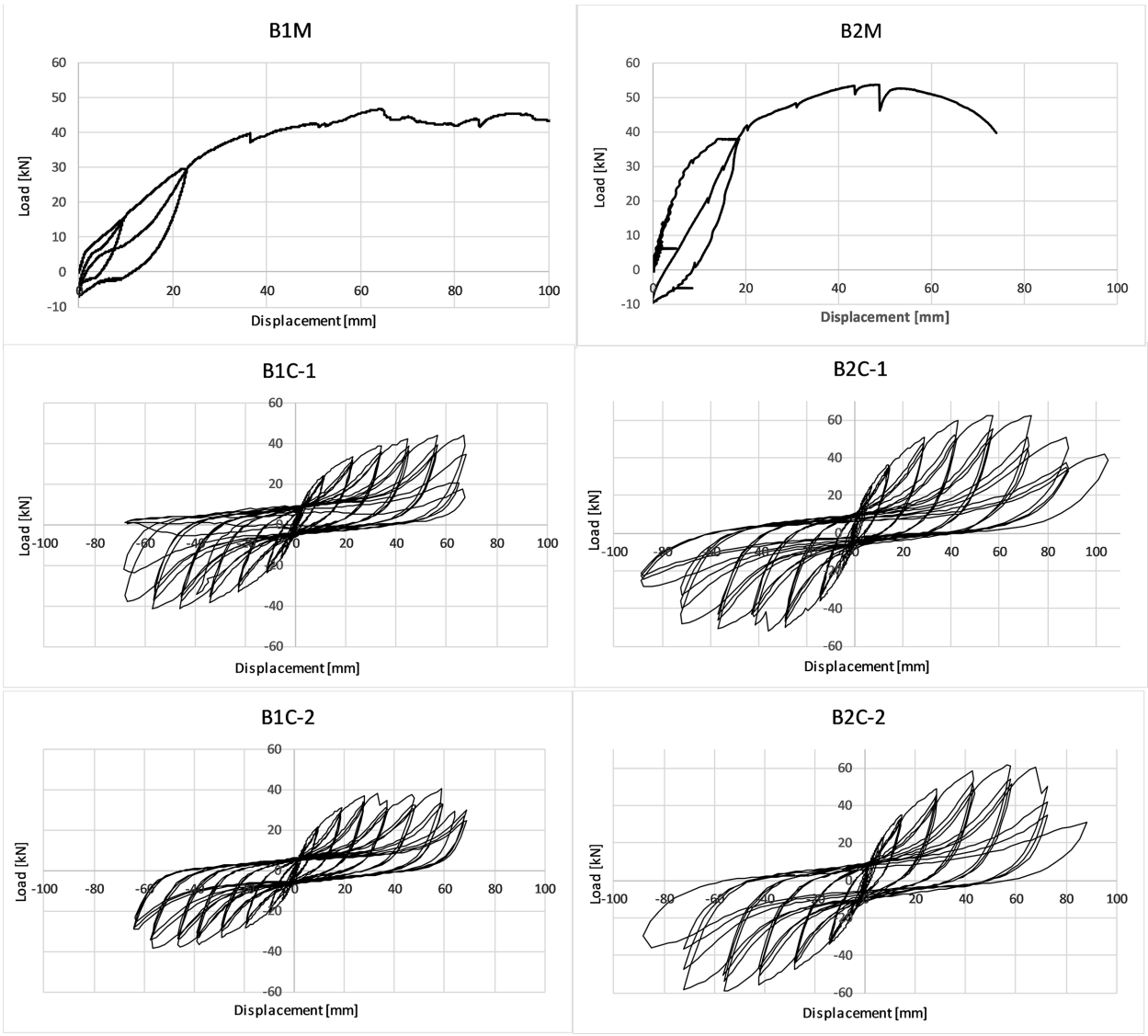

Fig. 6. Load – displacement curves for type B specimens.

3.4 Physical properties of materials

The moisture content and density of the wood frame and sheathing during testing is shown in TABLE III.

TABLE III
PHYSICAL PROPERTIES OF WOOD FRAME AND SHEATHING DURING TESTING

	Type A specimens		Type B specimens	
	Wood frame	Sheathing	Wood frame	Sheathing
Moisture content [%]	15.1	13.5	15.5	13.3
Density [kg/m^3]	532	513	420	549
Relative density	0.46	0.45	0.36	0.48
Oven-dry density [kg/m^3]	490	466	385	500
Oven-dry relative density	0.49	0.47	0.38	0.50

3.5 Failure modes

Fig. 7 shows the typical failure modes observed during testing. As can be seen, the most common failure mode for type A specimens is nail bending near the end posts where the stresses are higher (A1). In the case of type B specimens, the failure mode observed in all tests was panel withdrawal near the middle studs (B1). Furthermore, in a few cases, one of the end studs failed in tension (B2) and panel buckling at the compression end was also observed (B3).

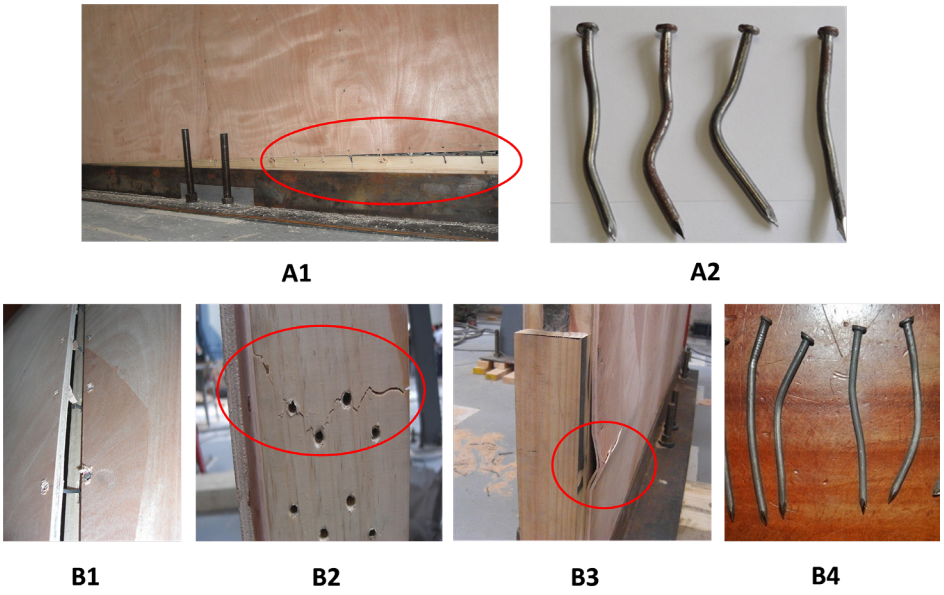

Fig. 7. Typical failure modes. A1: Nail bending and end stud uplift. A2: Deformed nails in type A specimens. B1: Panel withdrawal. B2: End stud failing in tension. B3: Panel buckling. B4: Deformed nails in type B specimens.

3.6 Theoretical calculations

In this section, the nominal shear strength (v_n), the design shear strength (v'), the apparent shear stiffness (G_a) and the deflection (δ_{sw}) of the wall will be estimated.

Shear strength

The shear strength will be estimated first by considering the lateral nail strength. Then, it will be estimated with table A.4.3A of AF&PA [1]. The lateral nail strength is estimated according to AF&PA [14]. Lateral nail strength depends on the oven-dry density of the frame and sheathing (G_{0m} and G_{0s} respectively), nail diameter (d), nail penetration in frame and sheathing (l_m and l_s, respectively) and nail yield bending (F_{yb}). First, the bearing strength for the frame and sheathing (F_{em} and F_{es}, respectively) are calculated with Eq. (6).

$$F_e = 114.5 G_0^{1.84} \tag{6}$$

For the frame: F_{em}=114.5(0.49)$^{1.84}$=30.8 MPa for type A specimen; F_{em}=114.5(0.38)$^{1.84}$=19.3 MPa for type B specimen. For the sheathing: F_{es}=114.5(0.47)$^{1.84}$=28.5 MPa for type A specimen;

F_{es}=114.5(0.50)$^{1.84}$=32.0 MPa for type B specimen; F_{yb}=620 MPa , d = 3.64 mm, l_m = 70-9 = 61 mm, l_s = 9 mm.

With these parameters, the nominal lateral nail strength is: Z_n = 1220 N for type A specimen and, Z_n = 1122 N for type B specimen. The failure mode is IIIs, in which a plastic hinge in the nail is formed in the main member (frame member), and the nail develops the bearing strength on both the main and side (sheathing) member.

The nominal unit shear strength can be obtained by dividing the nominal lateral nail strength by the nail spacing, and because there is sheathing on both sides, the value is multiplied by two:

$$v_n = \frac{2Z_n}{s} \tag{7}$$

$v_n = \frac{2(1220)}{0.15} = 16267\,\frac{\text{N}}{\text{m}} = 16.3$ kN/m for type A1 specimen; $v_n = \frac{2(1220)}{0.10} = 24400\,\frac{\text{N}}{\text{m}} = 24.4$ kN/m for type A2 specimen; $v_n = \frac{2(1122)}{0.15} = 14960\,\frac{\text{N}}{\text{m}} = 15.0$ kN/m for type B1 specimen; $v_n = \frac{2(1122)}{0.10} = 22440\,\frac{\text{N}}{\text{m}} = 22.4$ kN/m for type B2 specimen. The design strength v' is then obtained by multiplying the nominal value by 0.65 (connection strength factor, ϕ_z), see TABLE IV.

TABLE IV
UNIT SHEAR STRENGTH IN kN/m, ACCORDING TO TABLE A.4.3A OF REFERENCE [2] AND BASED ON NAIL STRENGTH (IN BRACKETS)

	Seismic		Wind	
Specimen	v_n	v'	v_n	v'
A1	12.4 [16.3]	9.92 [10.6]	17.4 [16.3]	13.9 [10.6]
A2	18.1 [24.4]	14.5 [15.9]	25.4 [24.4]	20.3 [15.9]
B1	11.3 [15.0]	9.04 [9.75]	15.8 [15.0]	12.6 [9.75]
B2	16.4 [22.4]	13.1 [14.6]	23.0 [22.4]	18.4 [14.6]

Apparent Shear Stiffness

The apparent shear stiffness, G_a, is also estimated with table A.4.3A of AF&PA [1]. The value for type A1 or B1 specimen is 2522 kN/m. The value for type A2 or B2 specimen is 3152 kN/m.

Shear wall deflection

Shear wall deflection, δ_{sw}, is calculated according to Eq. (8), see AF&PA [1].

$$\delta_{sw} = \frac{2}{3}\frac{v_u h^3}{EAb} + \frac{v_u h}{G_a} + \frac{h\Delta_a}{b} \tag{8}$$

Where: δ_{sw} is the shear wall deflection, mm. b is the shear wall length, mm. Δ_a is the total vertical elongation of wall anchorage system (including nail slip, anchorage device elongation, etc.) at the induced unit shear in the wall, mm. E is the modulus of elasticity of end studs, MPa. A is the area of end studs' cross section, mm^2. G_a is the apparent wall shear stiffness due to nail slip and panel shear deformation, kN/m. h is the shear wall height, mm. v_u is the induced unit shear in the wall, kN/m. With b = 2440 mm, E = 10 000 MPa, A = 40×90 = 3600 mm^2, G_a = 2522 kN/m or 3152 kN/m, h = 2440 mm:

$\delta_{sw}=0.11v_u+0.967v_u+\Delta_a$ for type A1 or B1 specimen and, $\delta_{sw}=0.11v_u+0.774v_u+\Delta_a$ for type A2 or B2 specimen. Taking the average maximum shear strengths, v_{max}, and the average yield strengths, v_y, the shear wall deformations are determined for both strengths and shown in TABLE V.

TABLE V
ESTIMATED SHEAR WALL DEFORMATIONS ACCORDING TO EQ. (8). Δ_a IS NOT INCLUDED

Specimen type	v_{max} [kN/m]	δ_{sw} [mm] at v_{max}	v_Y [kN/m]	δ_{sw} [mm] at v_Y
A1	8.36	9.01	7.47	8.07
A2	11.3	9.99	10.1	8.93
B1	17.6	19.0	15.5	16.7
B2	23.5	20.8	20.9	18.5

4. DISCUSSION

4.1 Type A specimen

As can be observed in Fig. 5, all the test specimens behaved in a similar way: approximately linear – elastic up to 30 – 40 % of the maximum load. After that point, the stiffness decreases as the deflection increases until the maximum load (zero stiffness) is reached. Then, the load drops as the deflection increases until failure occurs. As was described in the previous section, the failure is due to the bending of the nails, especially at the lower corners, near the end studs, where the vertical loads are high. Hence, it is noticeable that the structural behavior of the specimen is controlled by the connections between frame and sheathing. When comparing the monotonic and cyclic behavior, the monotonic curves correspond to the envelope curve of the first cycles of the cyclic curves (compare A1M with A1C-1 and A1C-2 and A2M with A2C-1 and A2C-2). The cyclic tests showed well-formed hysteresis loops, in which a load decrease occurs for the second and third cycle. A typical pinching effect was also observed, and it is due to the holes left by the nails bearing in the frame and sheathing, so when the loads are reversed, the stiffness is reduced until the nail bears against the frame and sheathing again. An average ductility factor of 4.6 was obtained from these specimens, implying energy dissipation and an adequate behavior for seismic action. The shear strength increased about 35 % when decreasing nail spacing from 150 mm to 100 mm. When comparing the estimated shear strength with the experimental values, the latter were lower. For A1 specimens, the experimental values were approximately 2.0 times lower than the estimated ones, considering the wind value and the nail strength value. For A2 specimens, the experimental values were approximately 2.2 times lower. This is because type A specimens do not have hold-down anchors, and hence, the capacity is diminished because the nails have to transfer the end studs' tension and compression forces. With these tests, it was confirmed that the estimated capacities are applicable when the end studs are anchored to the foundation. The experimental shear stiffness was also lower than the estimated ones, as was expected since the experimental shear stiffness includes bending deformation of the chords and uplift of the anchorage device. For type A1 specimen, the average experimental shear

stiffness was 14 % lower than the theoretical one, whereas for type A2 specimen, the average experimental shear stiffness was just 6.9 % lower. The hold-down anchors have less influence on the stiffness than on the strength. Finally, when comparing the estimated shear wall deflections (average of 9.5 mm) at maximum induced forces, they seem quite lower than the experimental ones. But multiplying these values by the ductility factor (9.5×4.6 = 43.7 mm) gives a more realistic and comparable value. The average experimental value is 49 mm so the approximate anchorage uplift (in this case nail slip) would be 49 - 43.7 = 5.3 mm. At yield strength level, the experimental values are 20-30 % higher.

4.2 Type B specimen

As can be observed in Fig. 6, all the type B specimens behaved in a similar way as the type A specimens. In the case of type B specimens, the failure, in most cases, is due to the nail lateral capacity and nail withdrawal at the panel edges as can be seen in Fig. 7 (B1). Other failure modes were also observed in a few cases, such as tension failure at the end stud and panel buckling (see Fig. 7 (B2) (B3)). When comparing the monotonic and cyclic behavior, it was the same as with type A specimens. The cyclic tests showed similar behavior than type A specimens as well. An average ductility factor of 5.3 was obtained from these specimens. The shear strength increased about 34 % when decreasing nail spacing from 150 mm to 100 mm. When comparing the estimated shear strength with the experimental values, there was a good agreement. For B1 specimens, the experimental values were approximately 11 % higher than the estimated ones, considering the wind value and the nail strength value. For B2 specimens, the experimental values were approximately 2 % higher. The experimental shear stiffness was also higher than the estimated ones. For type B1 specimen, the average experimental shear stiffness was 16 % higher than the theoretical one, whereas for type B2 specimen, the average experimental shear stiffness was 12 % higher. Finally, when comparing the estimated shear wall deflections (average of 19.9 mm) at maximum induced forces, they seem quite lower than the experimental ones. Multiplying these values by the ductility factor (19.9×5.3 = 105 mm) gives a higher value than the ones obtained experimentally (65 mm for specimens B1 and 76 mm for specimens B2). This difference is probably due to the estimated ductility factor. At yield strength level, the estimated value was 11 % higher for B1 specimen but for B2 specimen, the estimated value was 13 % lower.

4.3 General discussion

When comparing type A specimens with type B specimens, it was evident that type B specimens presented a better overall behavior than type A specimens. This confirms the importance of having hold-down anchors at the end studs of the wall. The shear strength of type B specimen was approximately 2.0 times that one of type A specimen. Type B specimen was also stiffer than type A specimen, 35 % stiffer for specimens with a nail spacing of 150 mm and 20 % stiffer for specimens with a nail spacing of 100 mm. The ductility factor was also higher for type B specimen (about 15% higher). However, as pointed before, the most relevant difference between the two types of specimens is the shear strength.

5. CONCLUSIONS

Wood frame shear walls constructed with available materials in Costa Rica can develop adequate shear strength and stiffness if the end studs are adequately anchored to the foundation.

All the specimens showed ductile behavior (ductility factors ranging from 3.7 to 6.3) which is important for energy dissipation during an earthquake.

The shear strength for type B specimen was higher than the nominal shear strength, which indicates that it can be safely designed with code specifications.

As expected, the shear strength for type A specimen was lower than the nominal strength, and hence, it is not recommended for its use as part of the lateral resisting system.

6. ROLE OF THE AUTHORS

The author Guillermo González Beltrán is responsible for the entire document.

ACKNOWLEDGEMENTS

This research was possible due to the sponsoring of the Costa Rican Seismic Code Commission and the National Laboratory for Materials and Structural Models (LANAMME) of the University of Costa Rica. A special acknowledgement to the research team: Bernardo Salas-Boraschi and Alejandro Robles-Field.

REFERENCES

[1] American Forest and Paper Association (AF&PA), *Special Design Provisions for Wind and Seismic with Commentary* (2005 ed.). Washington, DC, United States of America: AF&PA, Inc, 2005.

[2] European Committee for Standardization, Eurocode 5, *Design of Timber Structures. Part 1-1: General Rules and Rules for Buildings*. Brussels: CEN, 1993.

[3] B. Salas-Boraschi, Comportamiento estructural de paredes livianas con marco de madera y forro de madera contrachapada ante carga horizontal. San José, Costa Rica: Universidad de Costa Rica, 2010.

[4] B. Salas Boraschi and González, G., "*Comportamiento estructural de paredes livianas con marco de madera y forro de madera contrachapada ante carga horizontal,*" presented in XI Seminario de Ingeniería Estructural y Sísmica, San José, Costa Rica, 2011.

[5] A. Robles-Field, *Comportamiento estructural de paredes livianas con marco de madera y forro de madera contrachapada ante carga horizontal, con anclajes en la base*. San José, Costa Rica: Universidad de Costa Rica, 2013.

[6] A. Robles Field, and González, G. "Comportamiento estructural de paredes livianas con marco de madera y forro de madera contrachapada ante carga horizontal, con anclajes en la base," presented in XII Seminario de Ingeniería Estructural y Sísmica, San José, Costa Rica, 2013.

[7] J. M. Branco, F. T. Matos and P. B. Lourenço, "Experimental In-Plane Evaluation of Light Timber Walls Panels," *Buildings*, vol. 7, no. 3, p. 63, 2017, https://doi.org/10.3390/buildings7030063.

[8] K. Nagase, K. Kobayashi, and M. Yasumura, "Estimation of failure lifetime in plywood-to-timber joints with nails and screws under cyclic loading," *Buildings. Journal of Wood Science*, vol. 64, pp. 612–624, 2018, https://doi.org/10.1007/s10086-018-1742-8.

[9] R. L. Dhonju, "Racking Performance of Platform Timber Framed Walls", Doctoral dissertation, Edinburgh Napier University, 2018, http://researchrepository.napier.ac.uk/Output/2058930.

[10] S. Shadravan and C. Ramseyer, "Investigation of Wood Shear Walls Subjected to Lateral Load," *Structures*, vol. 16, pp. 82–96, 2018, https://doi.org/10.1016/j.istruc.2018.08.00.

[11] P. Orellana, H. Santa Maria, J. Almazán and X. Estrella, "Cyclic behavior of wood-frame shear walls with vertical load and bending moment for mid-rise timber buildings," *Engineering Structures*, vol. 240, p. 112298, 2021, https://doi.org/10.1016/j.engstruct.2021.112298.

[12] ASTM, ASTM E 564-06, "Standard Practice for Static Load Test for Shear Resistance of Framed Walls for Buildings," in *ASTM, Annual Book of ASTM Standards*. West Conshohocken: ASTM International, p. 5, 2006.

[13] ASTM, "Standard Test Methods for Cyclic (Reversed) Load Test for Shear Resistance of Vertical Elements of the Lateral Force Resisting Systems for Buildings," in *ASTM, Annual Book of ASTM Standards*. West Conshohocken: ASTM International, p. 13, 2005.

[14] American Forest and Paper Association (AF&PA), *National Design Specification for Wood Construction and Supplement*. Washington D.C.: AF&PA, 2005.

[15] Colegio Federado de Ingenieros y de Arquitectos de Costa Rica, *Código Sísmico de Costa Rica* 2010 4th ed. Cartago, Costa Rica: Editorial Tecnológica de Costa Rica, 2011.